KCNQ2 and KCNQ3 Potassium Channel Subunits: Molecular Correlates of the M-Channel

Hong-Sheng Wang, Zongming Pan, Wenmei Shi, Barry S. Brown, Randy S. Wymore, Ira S. Cohen, Jane E. Dixon,* David McKinnon

The M-current regulates the subthreshold electrical excitability of many neurons, determining their firing properties and responsiveness to synaptic input. To date, however, the genes that encode subunits of this important channel have not been identified. The biophysical properties, sensitivity to pharmacological blockade, and expression pattern of the KCNQ2 and KCNQ3 potassium channels were determined. It is concluded that both these subunits contribute to the native M-current.

The M-current is a slowly activating and deactivating potassium conductance that plays a critical role in determining the subthreshold electrical excitability of neurons as well as the responsiveness to synaptic inputs (*1*–*3*). The M-current was first described in peripheral sympathetic neurons (*4*, *5*), and differential expression of this conductance produces subtypes of sympathetic neurons with distinct firing patterns (*3*). The M-current is also expressed in many neurons in the central nervous system (CNS) (*1*, *6*, *7*).

To date, the molecular identity of the channels underlying the M-current remains unknown. Here we show that the KCNQ2 and KCNQ3 channel subunits can coassemble to form a channel with essentially identical biophysical properties and pharmacological sensitivities to the native M-current and that the pattern of *KCNQ2* and *KCNQ3* gene expression is consistent with these genes encoding the native M-current.

The KCNQ potassium channel gene family has three members: KCNQ1 (KvLQT1), KCNQ2, and KCNQ3 (*8*–*12*). Injection of KCNQ2 mRNA into *Xenopus* oocytes resulted in the consistent expression of a relatively small potassium current that is slowly activating and deactivating (Fig. 1A). The properties of this channel are essentially identical to those described previously (*11*). In contrast, injection of KCNQ3 mRNA did not result in the expression of a current above background level. When the KCNQ2 and KCNQ3 mRNAs were coinjected, however, the resultant current was 11-fold larger than that found in cells injected with KCNQ2 mRNA alone (Fig. 1, A and B). The large increase in current density after coinjection of KCNQ3 mRNA suggests that the KCNQ3 subunit facilitates expression of the KCNQ2 subunits, possibly by the formation of a heteromeric complex of KCNQ2 and KCNQ3 subunits. Expression of a relatively small current after KCNQ3 mRNA injection into oocytes has been reported (*13*), suggesting that the KCNQ3 subunit can function as a homomeric channel under some experimental conditions. It is possible, however, that assembly with the endogenous *Xenopus* KCNQ subunit (*14*) may facilitate KCNQ3 expression in these experiments.

In addition to affecting current density, the KCNQ3 subunit affects the sensitivity of the KCNQ2 channel to blockade by tetraethylammonium (TEA). The homomultimeric KCNQ2 channel was very sensitive to TEA [dissociation constant (K_d) = 0.16 ± 0.02 mM, n = 5], whereas channels expressed after coinjection of KCNQ2 and KCNQ3 mRNAs were much less sensitive (K_d = 3.5 ± 0.7 mM, n = 6). The KCNQ2 and KCNQ3 subunits differ within the pore region, at a position that determines sensitivity to blockade by TEA (Fig. 1C). The KCNQ2 subunit has a tyrosine residue at this position, which confers high sensitivity to TEA, whereas the KCNQ3 channel has a threonine residue, which confers low sensitivity to TEA (*15*). The intermediate sensitivity to TEA block of the KCNQ2+KCNQ3 channels confirms that the KCNQ2 and KCNQ3 subunits coassemble into a heteromultimeric complex (Fig. 1D), in a manner closely analogous to heteromultimers of *Shaker* channels (*16*). For comparison, the native M-current in rat sympathetic neurons is also moderately sensitive to blockade by TEA [median inhibitory concentration (IC_{50}) = 5.8 ± 0.2 mM, n = 3], as is the M-current found in hippocampal and olfactory cortex neurons (*6*). It seems likely, therefore, that if the KCNQ2 and KCNQ3 subunits contribute to the native M-channel, they assemble as a heteromultimeric complex with expression of both subunits required to achieve normal current levels and pharmacological properties.

The kinetic properties of the KCNQ2+KCNQ3 channel were markedly similar to

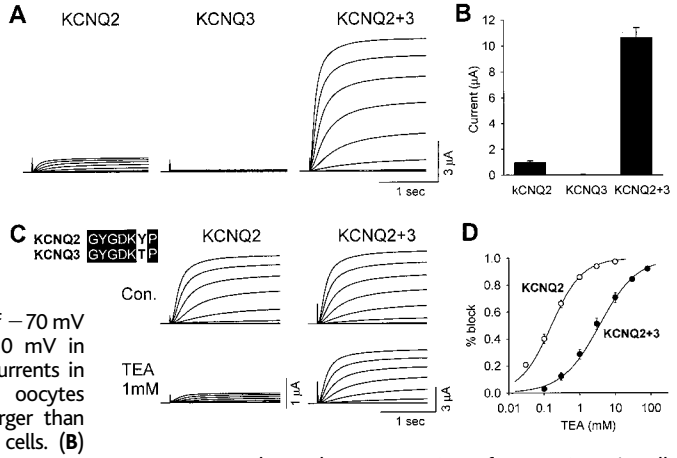

Fig. 1. The KCNQ2 and KCNQ3 potassium channel subunits form heteromultimers. (**A**) Currents recorded in *Xenopus* oocytes after injection of KCNQ2 mRNA, KCNQ3 mRNA, or an equimolar ratio of KCNQ2 and KCNQ3 mRNAs (*30*, *31*). Currents elicited by 2-s voltage steps from a holding potential of −70 mV over the range −60 to 0 mV in 10-mV increments. The currents in KCNQ3 mRNA–injected oocytes were not substantially larger than those seen in uninjected cells. (**B**) Histogram showing the average current response to a voltage-clamp step to 0 mV from −70 mV in cells injected with KCNQ2, KCNQ3, or an equimolar ratio of KCNQ2 and KCNQ3 mRNAs (45 ng of each mRNA was injected per oocyte). Average current responses in the three sets of cells were significantly different to each other ($P < 0.001$, n = 19 to 22). (**C**) Effect of 1 mM TEA on currents elicited from oocytes injected with KCNQ2 mRNA or an equimolar ratio of KCNQ2 and KCNQ3 mRNAs. The voltage clamp protocol was the same as that used in (A). The KCNQ2+KCNQ3 mRNA mixture was diluted to reduce current density. (**Inset**) Comparison of the deduced amino acid sequence in the pore region around the residue controlling TEA sensitivity [equivalent to position 449 in the *Shaker* H4 channel (*16*)]. D, Asp; G, Gly; K, Lys; P, Pro; T, Thr; Y, Tyr. (**D**) Dose-response curves for TEA block of KCNQ2 channels and KCNQ2+KCNQ3 channels. Figure shows averaged data fitted with the Hill equation with average parameters obtained from fits to individual cells. For KCNQ2, K_d = 0.16 ± 0.02 mM (n = 5) and the Hill coefficient was set to unity. For KCNQ2+KCNQ3, K_d = 3.5 ± 0.7 mM, Hill coefficient = 0.82 ± 0.03 (n = 6).

H.-S. Wang, R. S. Wymore, I. S. Cohen, J. E. Dixon, Institute of Molecular Cardiology, Department of Physiology and Biophysics, State University of New York at Stony Brook, Stony Brook, NY 11794, USA. Z. Pan, W. Shi, D. McKinnon, Department of Neurobiology and Behavior, State University of New York at Stony Brook, Stony Brook, NY 11794, USA. B. S. Brown, CNS Diseases Research, DuPont Pharmaceuticals, Wilmington, DE 19880, USA.

*To whom correspondence should be addressed.

those of the native M-current. Characteristic kinetic properties of the M-current include a relatively negative activation curve, a substantial steady-state conductance at −30 mV, and slow activation and deactivation kinetics (*3*, *5*). By use of the classic M-current voltage-clamp protocol (*4*), the KCNQ2+KCNQ3 channel closely replicated the waveform of the native M-current (Fig. 2A). The activation waveform was similar for the two currents, although the native current appeared to activate slightly faster (Fig. 2B). The conductance-voltage curves were very similar for the two channel types with the threshold for activation near −60 mV and most of the channels activated at −30 mV (Fig. 2C). The deactivation kinetics of the M-current are biphasic (*17*), and this was also true for the KCNQ2+KCNQ3 channel (Fig. 2D). Both channel types had similar time constants for the two components of deactivation. Deactivation time constants at −50 mV for the M-current were 145 ± 25 ms and 838 ± 125 ms (fast component, 55 ± 3% of total; n = 4), and for KCNQ2+KCNQ3 were 171 ± 12 ms and 857 ± 146 ms (fast component, 49 ± 3%; n = 9). At −60 mV these values were, for the M-current, 126 ± 28 ms and 934 ± 117 ms (fast component, 60 ± 2%; n = 4), and for KCNQ2+KCNQ3, 149 ± 9 ms and 741 ± 69 ms (fast component, 59 ± 3%; n = 9). For both the native M-current and the KCNQ2+KCNQ3 channels, the time constant of the fast component was voltage sensitive (Fig. 2E), whereas the slow component was relatively insensitive to voltage over the same voltage range.

Although the kinetic properties of the KCNQ2+KCNQ3 channel were very similar to those of the native M-current, it is important to establish other criteria that can be used to determine the molecular identity of the native conductance. One obvious approach is to determine the sensitivity of candidate channels to muscarinic inhibition, the characteristic that gives the M-current its name. We find that the KCNQ2+KCNQ3 channel is strongly inhibited by muscarine when coexpressed in *Xenopus* oocytes with the m_1 muscarinic receptor (*18*). This criterion is too broad to be very useful for at least two reasons. First, a wide range of potassium currents in addition to the M-current are inhibited in sympathetic neurons after muscarinic receptor stimulation (*19*). Second, many different cloned potassium channels are inhibited after stimulation of coexpressed m_1 muscarinic receptors. The M-current is sensitive to blockade by Ba^{2+} ions (*1*) and the KCNQ2+KCNQ3 channel is similarly sensitive (67 ± 3% block by 1 mM Ba^{2+}, n = 5). This criterion is also too broad, however, with many other potassium channels showing a similar sensitivity to Ba^{2+} ions.

Another approach is the use of selective blocking drugs. Two drugs that are useful in establishing the identity of the M-channel are linopirdine and 10,10-*bis*(4-pyridinylmethyl)-9(10 H)-anthracenone (XE991) (*20*). Linopirdine blocks the M-current at micromolar concentrations by direct channel blockade (*21*–*23*). The IC_{50} for block of the M-channel in sympathetic neurons by linopirdine is in the range 3.4 to 7.0 μM (*22*, *23*).

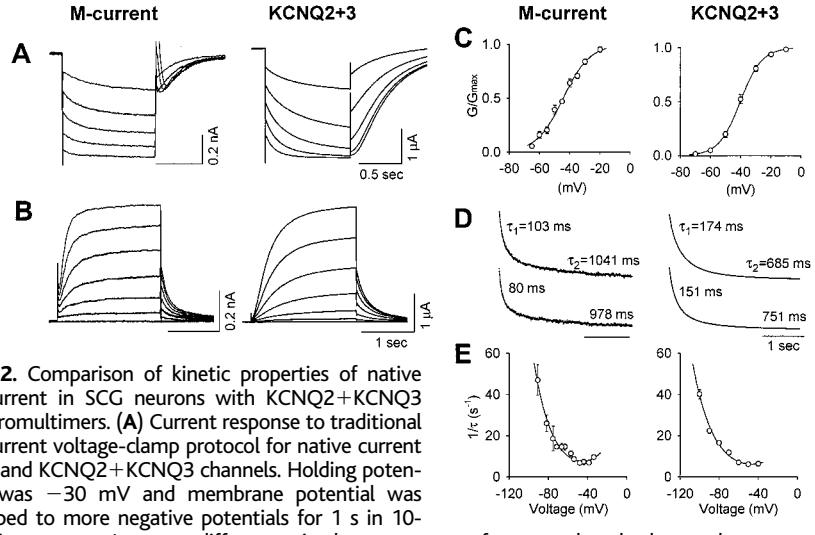

Fig. 2. Comparison of kinetic properties of native M-current in SCG neurons with KCNQ2+KCNQ3 heteromultimers. (**A**) Current response to traditional M-current voltage-clamp protocol for native current (*32*) and KCNQ2+KCNQ3 channels. Holding potential was −30 mV and membrane potential was stepped to more negative potentials for 1 s in 10-mV increments. Apparent differences in the current waveforms are largely due to the presence of a linear leak current in the recordings from SCG neurons that is relatively smaller in the oocytes. The initial phase of M-current reactivation in SCG neurons is obscured by activation of the A-current. (**B**) Activation of M-current and KCNQ2+KCNQ3 channels from a holding potential of −60 mV in 5-mV increments. (**C**) Conductance-voltage curves fitted with a single Boltzmann function. For the native M-current the fit is to averaged data points, with V_n = −44 mV and k_n = −8.8 mV (n = 6, bars are SEMs). For KCNQ2+KCNQ3 channels, V_n = −40 ± 1 mV and k_n = −6.8 ± 0.1 mV (n = 6, bars are SEMs). Conductance-voltage curves for KCNQ2+KCNQ3 channels were constructed with tail currents at −60 mV after depolarizing voltage steps from a holding potential of −70 mV. (**D**) Deactivation process had two time constants for both channel types. Time constants for deactivation are shown next to current traces for steps from −30 mV holding potential to −50 mV (top trace) or −60 mV. Biexponential fits are superimposed on the experimental data. (**E**) Reciprocal time constant for fast deactivation of the native M-current and KCNQ2+KCNQ3 channels. Data points are averages from three to nine cells for the native M-current and nine cells for KCNQ2+KCNQ3. Data were fitted with the equation (*5*) $1/\tau = \alpha_0(\beta_0) \exp[\pm(V_m - V_0)/y]$, where V_m is the membrane potential, $\alpha_0(\beta_0)$ = 3.8 s^{-1}, V_0 = −45.4 mV, and y = 18.3 mV for the native M-current and $\alpha_0(\beta_0)$ = 3.0 s^{-1}, V_0 = −46.7 mV, and y = 20.9 mV for the KCNQ2+KCNQ3 channel. The native M-current was recorded from SCG neurons in intact, isolated ganglia and the KCNQ2+KCNQ3 currents were recorded in *Xenopus* oocytes, both at room temperature.

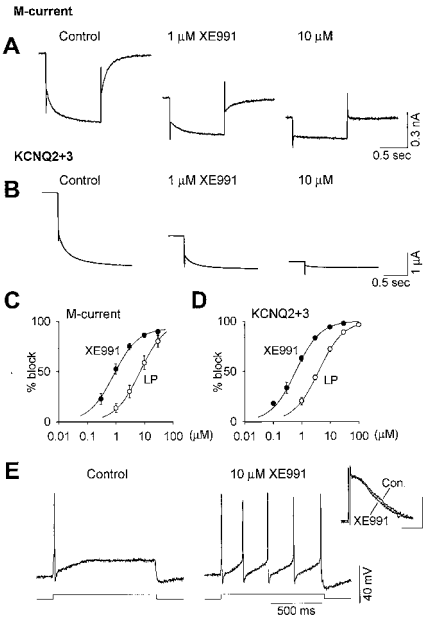

Fig. 3. Channel blockade by XE991 of the M-current and KCNQ2+KCNQ3 channels. (**A**) Blockade of M-current in SCG neurons by XE991. Holding potential was −30 mV and step potential was −50 mV for 1 s. The shift in holding current after drug application is due to the inhibition of M-current activated at the holding potential. (**B**) Blockade of KCNQ2+KCNQ3 channels by XE991. Holding potential was −60 mV and the cell was repetitively depolarized to −30 mV for 1 min to reach steady-state blockade. Tail currents were recorded at −60 mV. (**C** and **D**) Dose-response curves for linopirdine (○) and XE991 (●) for blockade of M-current (C) and KCNQ2+KCNQ3 channels (D). Maximal block was 93 ± 2% of native M-current and 100% of KCNQ2+KCNQ3 channels. Data points are averages and error bars represent SEMs. (**E**) Effect of 10 μM XE991 on the firing properties of a phasic sympathetic neuron recorded from the SCG. Membrane potential was held at −60 mV and the depolarizing current step was 0.2 nA for control and XE991 application. (**Inset**) Voltage-clamp recording of the I_{AHP} before and after application of 10 μM XE991. Recordings were done as described (*3*). Calibration bar, 200 ms and 0.1 nA.

The related compound XE991 has an IC_{50} of 0.98 ± 0.15 μM (Fig. 3C). Only one class of voltage-gated potassium channels had a pharmacological profile similar to that of the native M-current: the KCNQ channels, which were blocked by both XE991 and linopirdine at very similar concentrations to the native M-current (Table 1). Of particular interest was XE991, which had both high affinity and selectivity for the native M-channel and KCNQ channels. No *eag*- or *Shaker*-related channel tested had a similar sensitivity. Unlike the KCNQ2 and KCNQ3 channels, the KCNQ1 channel cannot contribute to the native M-channel because the *KCNQ1* gene is not expressed in either sympathetic ganglia (*24*) or the CNS (*8*).

Consistent with the high selectivity of XE991 for the M-current is its effect on the firing properties of sympathetic neurons. In the rat, there are two classes of sympathetic neurons: phasic-firing neurons, which have a relatively large M-current, and tonic-firing neurons, which do not express an M-current (*3*). We have shown previously that differential expression of the M-current is the primary determinant of the different firing properties of phasic and tonic neurons (*3*). This conclusion is confirmed by the observation that blocking the M-current in phasic neurons with 10 μM XE991 converts the firing properties from phasic to tonic without affecting any other electrophysiological properties, including the slow after-hyperpolarization (Fig. 3E).

The expression pattern of *KCNQ2* and *KCNQ3* genes in sympathetic ganglia is consistent with these genes encoding subunits of the M-channel. The expression of multisubunit proteins is often regulated by limiting the expression of a single subunit, and this is apparently true for the M-current. The superior cervical ganglia (SCG) contain only phasic neurons, whereas the prevertebral sympathetic ganglia (celiac ganglia and superior mesenteric ganglia) contain predominantly tonic neurons (Fig. 4A). The gene regulating expression of the M-channel should, therefore, be expressed at substantially lower levels in prevertebral sympathetic ganglia than in the SCG, and *KCNQ2* gene expression does in fact closely parallel M-current expression in these ganglia (Fig. 4B). Of the 24 different voltage-gated potassium channel genes tested to date, no other gene has a similar expression pattern in sympathetic ganglia (*25*, *26*). The *KCNQ3* gene was expressed at approximately equal levels in both SCG and prevertebral ganglia (Fig. 4C). The KCNQ3 subunit expresses poorly or not at all when expressed by itself in vitro and it is likely, therefore, that M-current expression in sympathetic ganglia is determined primarily by regulation of *KCNQ2* gene expression.

In the CNS, the M-current is expressed in many neurons in the cortex and hippocampus but has not been described in the cerebellum. In contrast to the peripheral nervous system, *KCNQ2* gene expression does not parallel M-current expression in these CNS regions, and the *KCNQ2* gene was expressed at relatively high levels in all three regions (Fig. 4D). The *KCNQ3* gene, however, was expressed at much lower levels in the cerebellum than in cortex and hippocampus, like the M-current (Fig. 4E), suggesting that regulation of *KCNQ3* gene expression is also important in determining M-current expression levels in vivo. This conclusion is consistent with the in vitro results demonstrating that expression of the KCNQ2+KCNQ3 heteromultimeric channel is much more efficient than that of the KCNQ2 homomultimer.

Taken together, these results strongly suggest that the KCNQ2 and KCNQ3 subunits contribute to the native M-channel. The KCNQ2+KCNQ3 channel is the only known potassium channel that can reproduce the unique kinetic properties of the native M-cur-

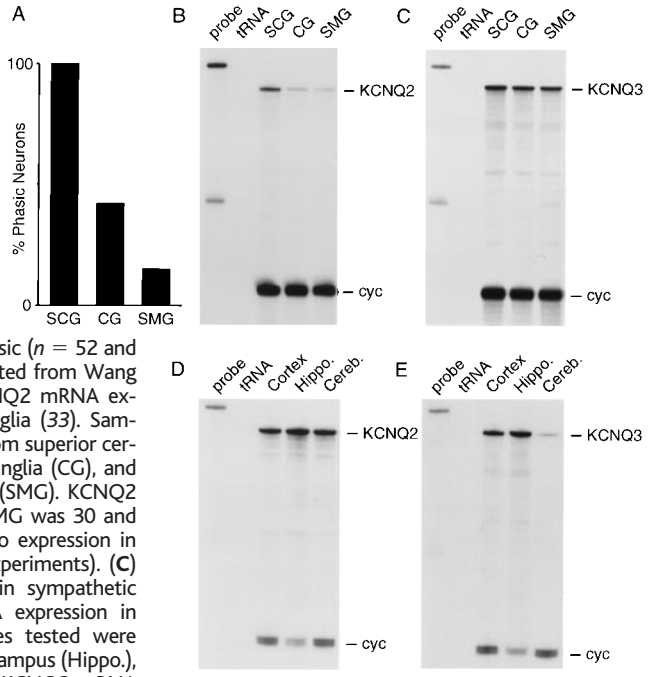

Fig. 4. KCNQ2 and KCNQ3 mRNA expression in different rat sympathetic ganglia and brain regions determined by RNase protection analysis. (**A**) Histogram showing the distribution of phasic neurons in prevertebral and paravertebral sympathetic ganglia. Neurons in SCG are exclusively phasic (n = 36), whereas only 42% of the neurons in the CG and 15% in SMG are phasic (n = 52 and 40, respectively). [Data adapted from Wang and McKinnon (*3*).] (**B**) KCNQ2 mRNA expression in sympathetic ganglia (*33*). Samples tested were prepared from superior cervical ganglia (SCG), celiac ganglia (CG), and superior mesenteric ganglia (SMG). KCNQ2 expression in the CG and SMG was 30 and 19%, respectively, relative to expression in the SCG (average of two experiments). (**C**) KCNQ3 mRNA expression in sympathetic ganglia. (**D**) KCNQ2 mRNA expression in three brain regions. Samples tested were prepared from cortex, hippocampus (Hippo.), and cerebellum (Cereb.). (**E**) KCNQ3 mRNA expression in three brain regions. All samples contained 5 μg of total RNA, and the cyclophilin gene (cyc) was used as a positive internal control and yeast tRNA as a negative control.

Table 1. Comparison of M-current and cloned potassium channels: IC_{50} for linopirdine and XE991 blockade. The number of cells is indicated in parentheses. IC_{50} values (mean ± SEM) are expressed in micromolar. In cases where the IC_{50} values were >100 μM, the exact value is not reported owing to limited solubility of the drug. It has been suggested that *eag*-related potassium channels might encode the M-current (*29*), and all the *eag*-related channels expressed in SCG (*26*) were tested in addition to representative examples of delayed-rectifier and A-channels.

M-current	KCNQ2 +KCNQ3	KCNQ2	KCNQ1	eag1	erg1	erg3	elk1	Kv1.2	Kv4.3
XE991									
0.98 ± 0.15 (3)	0.6 ± 0.1 (6)	0.71 ± 0.07 (6)	0.75 ± 0.05 (7)	49 ± 6* (6)	>100 (4)	>100 (6)	>100 (5)	>100 (5)	43 ± 7 (5)
Linopirdine									
7.0 ± 1.1† (5)	4.0 ± 0.5 (6)	4.8 ± 0.6 (5)	8.9 ± 0.9 (6)	31 ± 3* (9)	53 ± 4 (6)	85 ± 5 (5)	37 ± 4‡ (7)	68 ± 6 (4)	86 ± 14 (4)

*Blockade of the eag1 channel was incomplete with 82 ± 1% (n = 4) blockade by 1 mM linopirdine and 56 ± 2% (n = 6) blockade by 100 μM XE991. †Data adapted from Costa and Brown (*23*); a similar value of 3.4 ± 0.3 μM was obtained by Lamas *et al.* (*22*). ‡The IC_{50} for block of elk1 channels by linopirdine was highly voltage dependent, and the value shown is for a step to −10 mV. IC_{50} values ranged from 26 ± 3 μM at −20 mV (n = 7) to 144 ± 10 μM at +30 mV (n = 3).

rent, and several different pharmacological agents have very similar effects on the native M-current and the KCNQ2+KCNQ3 channel. In particular, the compound XE991 is highly selective for both the M-current and KCNQ channels. Finally, the *KCNQ2* gene is the only known potassium channel gene that is expressed in a pattern that parallels the distribution of the M-current in peripheral sympathetic ganglia. These data make a compelling case for the hypothesis that the KCNQ2+KCNQ3 channel is a molecular correlate of the M-current in sympathetic neurons.

The *KCNQ2* and *KCNQ3* genes are also abundantly expressed in the CNS, and it is likely that the KCNQ2+KCNQ3 subunits contribute to the M-current in central neurons. This conclusion is consistent with the observation that mutations in either the *KCNQ2* or *KCNQ3* genes result in an inherited autosomal dominant epilepsy (*10*–*12*). The very similar phenotypes produced by mutations in either of these two distinct genes (*27*) can be explained by the observation that both gene products are required to produce full expression of functional channels. Identification of the physiological function of the channel encoded by the *KCNQ2* and *KCNQ3* genes may facilitate the development of symptomatic treatments for these epilepsies.

References and Notes

1. D. A. Brown, in *Ion Channels*. T. Narahashi, Ed. (Plenum, New York, 1988), pp. 55–94.
2. W. M. Yamada, C. Koch, P. R. Adams, in *Methods in Neuronal Modeling*, C. Koch and I. Segev, Eds. (Bradford, Cambridge, MA, 1989), pp. 97–133.
3. H.-S. Wang and D. McKinnon, *J. Physiol.* **485**, 319 (1995).
4. D. A. Brown and P. R. Adams, *Nature* **283**, 673 (1980).
5. A. Constanti and D. A. Brown, *Neurosci. Lett.* **24**, 289 (1981).
6. J. F. Storm, *J. Physiol.* **409**, 171 (1989); A. Constanti and J. A. Sim, *ibid.* **387**, 173 (1987).
7. M. D. Womble and H. C. Moises, *ibid.* **457**, 93 (1992).
8. Q. Wang *et al.*, *Nature Genet.* **12**, 17 (1996).
9. A. Wei, T. Jegla, L. Salkoff, *Neuropharmacology* **35**, 805 (1996).
10. N. A. Singh *et al.*, *Nature Genet.* **18**, 25 (1998).
11. C. Biervert *et al.*, *Science* **279**, 403 (1998).
12. C. Charlier *et al.*, *Nature Genet.* **18**, 53 (1998).
13. Yang *et al.*, *J. Biol. Sci.* **273**, 19419 (1998).
14. M. C. Sanguinetti *et al.*, *Nature* **384**, 80 (1996).
15. R. MacKinnon and G. Yellen, *Science* **250**, 276 (1990).
16. L. Heginbotham and R. MacKinnon, *Neuron* **8**, 483 (1992).
17. N. V. Marrion, P. R. Adams, W. Gruner, *Proc. R. Soc. London Ser. B* **248**, 207 (1992).
18. H.-S. Wang *et al.*, data not shown. KCNQ2, KCNQ3, and m_1 muscarinic receptor mRNAs were coinjected, and inhibition after application of 10 μM muscarine was measured.
19. J. F. Cassell and E. M. McLachlan, *Br. J. Pharmacol.* **91**, 259 (1987); H.-S. Wang and D. McKinnon, *J. Physiol.* **492**, 467 (1996).
20. R. Zaczek *et al.*, *J. Pharmacol. Exp. Ther.* **285**, 724 (1998).
21. S. P. Aiken, B. J. Lampe, P. A. Murphy, B. S. Brown, *Br. J. Pharmacol.* **115**, 1163 (1995).
22. J. A. Lamas, A. A. Selyanko, D. A. Brown, *Eur. J. Neurosci.* **9**, 605 (1997).
23. A. M. N. Costa and B. S. Brown, *Neuropharmacology* **36**, 1747 (1997).
24. H.-S. Wang *et al.*, data not shown. Ribonuclease (RNase) protection assay of SCG RNA was done with a rat KCNQ1-specific probe.
25. J. E. Dixon and D. McKinnon, *Eur. J. Neurosci.* **8**, 183 (1996).
26. W. Shi *et al.*, *J. Neurosci.* **17**, 9423 (1997); W. Shi *et al.*, *J. Physiol.* **511**, 675 (1998).
27. O. Steinlein *et al.*, *Hum. Genet.* **95**, 411 (1995).
28. J. E. Dixon *et al.*, *Circ. Res.* **79**, 659 (1996).
29. C. E. Stansfeld *et al.*, *Trends Neurosci.* **20**, 13 (1997).
30. The *KCNQ3* gene was initially identified as an expressed sequence tag in a search of GenBank (accession number AA001392). On the basis of this sequence, primers were designed and used to amplify partial KCNQ3 cDNA clones from rat brain and SCG cDNA by polymerase chain reaction (PCR). We determined an initial sequence encompassing the entire open reading frame of the *KCNQ3* gene by performing several rounds of 5′ and 3′ RACE (rapid amplification of cDNA ends) PCR using initial anchor oligonucleotides complementary to the partial cDNA clone and SCG cDNA as a template for amplification. Once cDNAs were obtained that extended beyond both the 5′ and 3′ ends of the open reading frame, oligonucleotides complementary to noncoding regions at either end of the coding sequence were designed. We amplified multiple full-length cDNA clones in independent PCR reactions from rat SCG cDNA using Expand Long Template PCR (Boehringer Mannheim, Indianapolis, IN) with several combinations of the following oligonucleotides: TTGACTCCCCATCCGACCT and GCCTTTGCCTTCTTTTGGG (forward reaction), and ACCGCGCACATGCATG and GTGACATGGGGAGGAAGAA (reverse reaction). Four independent clones were sequenced in their entirety in both directions by automatic sequencing (GenBank accession number AF091247). The deduced amino acid sequence was 95% identical to a recently described partial human KCNQ3 cDNA clone (*12*).
31. We amplified full-length KCNQ2 cDNAs from adult human brain cDNA using primers CCCCGCTGAGCCTGAG and TGTAAAAGGTCACTGCCAGG with the Expand High Fidelity enzyme mixture (Boehringer Mannheim). The KCNQ2 cDNA clone used in the biophysical studies was identical to the KCNQ2 cDNA isolated previously from a fetal brain cDNA library (*10*) with the exception of a small deletion in the carboxy intracellular domain (30 amino acids from residues 417 to 446). This region is also alternatively spliced in the KCNQ2 cDNA clone described by Biervert *et al.* (*11*). Preparation, injection of complementary RNA, and recording from oocytes were done as described (*28*). The standard extracellular recording solution contained 82 mM NaCl, 2 mM KCl, 1.8 mM $CaCl_2$, 1 mM $MgCl_2$, and 5 mM Na-Hepes (pH 7.6). Data collection and analysis were done with pClamp software (Axon Instruments, Foster City, CA).
32. Recordings of the M-current in sympathetic neurons in intact ganglia were done at room temperature as described (*3*). The standard extracellular recording solution contained NaCl (133 mM), KCl (4.7 mM), NaH_2PO_4 (1.3 mM), $NaHCO_3$ (16.3 mM), $CaCl_2$ (2 mM), $MgCl_2$ (1.2 mM), and glucose (1.4 g/liter) in an atmosphere of 95% O_2–5% CO_2 to give pH 7.2 to 7.4. Linopirdine and XE991 were from DuPont Pharmaceuticals (Wilmington, DE).
33. Preparation of RNA, RNase protection assays, and isolation of a specific rat KCNQ2 and KCNQ3 probes were done as described (*25*). RNA expression was quantitated directly from dried gels with a PhosphorImager (Molecular Dynamics, Sunnyvale, CA).

34. We thank P. Adams for help and support throughout the course of this work, J. Keast for comments on the manuscript, P. McKinnon for technical assistance, and the anonymous reviewers for suggestions. Supported by grants from the National Institutes of Health.

17 June 1998; accepted 27 October 1998

Linkage of ATM to Cell Cycle Regulation by the Chk2 Protein Kinase

Shuhei Matsuoka, Mingxia Huang, Stephen J. Elledge*

In response to DNA damage and replication blocks, cells prevent cell cycle progression through the control of critical cell cycle regulators. We identified Chk2, the mammalian homolog of the *Saccharomyces cerevisiae* Rad53 and *Schizosaccharomyces pombe* Cds1 protein kinases required for the DNA damage and replication checkpoints. Chk2 was rapidly phosphorylated and activated in response to replication blocks and DNA damage; the response to DNA damage occurred in an ataxia telangiectasia mutated (ATM)–dependent manner. In vitro, Chk2 phosphorylated Cdc25C on serine-216, a site known to be involved in negative regulation of Cdc25C. This is the same site phosphorylated by the protein kinase Chk1, which suggests that, in response to DNA damage and DNA replicational stress, Chk1 and Chk2 may phosphorylate Cdc25C to prevent entry into mitosis.

When DNA is damaged, cells activate a response pathway that arrests the cell cycle and induces the transcription of genes that facilitate repair. The failure of this response results in genomic instability, a mutagenic condition that predisposes organisms to cancer. In eukaryotes, this checkpoint pathway initiated by DNA damage consists of several protein kinases, including the phosphoinositide kinase (PIK) homologs ATM, ATR, Mec1, and Rad3 and the protein kinases Rad53, Cds1, Chk1, and Dun1 (*1*). In mammals, in response to DNA damage, ATM controls cell cycle arrest in G_1 and G_2 and also prevents ongoing DNA synthesis (*1*). ATM controls G_1 arrest by activation of p53 (*2*), which induces transcription of the Cdk

Howard Hughes Medical Institute, Verna and Marrs McLean Department of Biochemistry and Department of Molecular and Human Genetics, Baylor College of Medicine, One Baylor Plaza, Houston, TX 77030, USA.

*To whom correspondence should be addressed. E-mail: selledge@bcm.tmc.edu